GRAPHICAL ABSTRACT

Molecular architecture manipulation in free radical copolymerization: An advanced Monte Carlo approach to screening copolymer chains with various comonomer sequence arrangements

Mohammad Reza Saeb, Yousef Mohammadi, Amir Saeid Pakdel, Alexander Penlidis

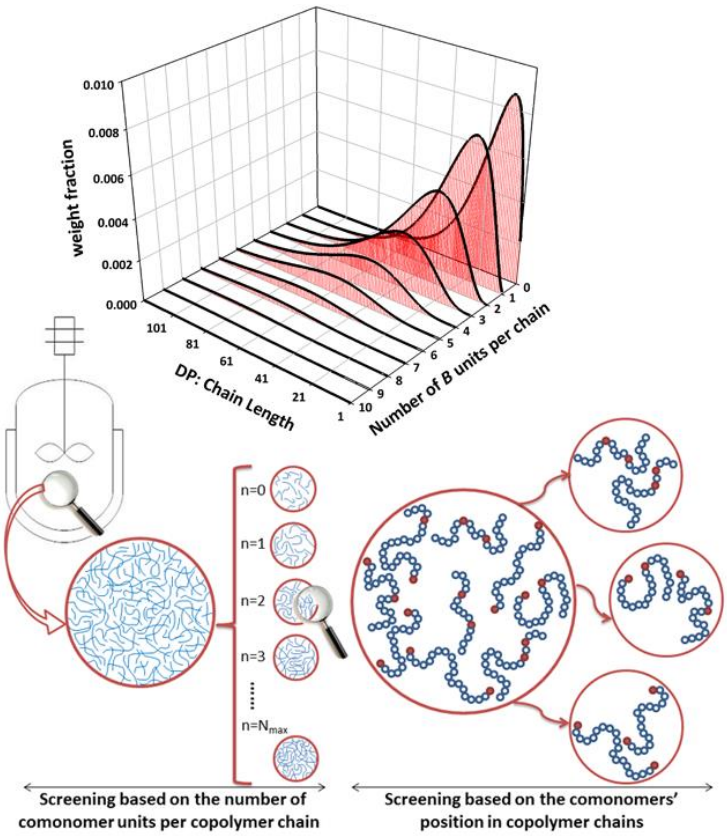

Molecular architecture manipulation in free radical copolymerization: An advanced Monte Carlo approach to screening copolymer chains with various comonomer sequence arrangements

Mohammad Reza Saeb[1], Yousef Mohammadi[2*], Amir Saeid Pakdel[1], Alexander Penlidis[3*]

1 Department of Resin and Additives, Institute for Color Science and Technology, P.O. Box 16765-654, Tehran, Iran

2 Petrochemical Research and Technology Company (NPC-rt), National Petrochemical Company (NPC), P.O. Box 14358-84711, Tehran, Iran

3 Department of Chemical Engineering, Institute for Polymer Research (IPR), University of Waterloo, Waterloo, Ontario, Canada N2L 3G1

To whom correspondence may be addressed:

Alexander Penlidis, penlidis@uwaterloo.ca

Yousef Mohammadi, mohammadi@npc-rt.ir

ABSTRACT

A Kinetic Monte Carlo (KMC) simulation approach was adopted in this study to capture evolutionary events in the course of free radical copolymerization, through which batch and starved-feed semibatch processes were compared. The implementation of the KMC code developed in this work: (*i*) enables satisfactory control of the molecular weight of the copolymer by tracking the profiles of concentrations of macroradicals, monomers, and polymer as well as degree of polymerization, polydispersity, and chain length distribution; (*ii*) captures the bivariate distribution of chain length and copolymer composition; (*iii*) comprehensively tracks and analyzes detailed information on the molecular architecture of the growing chains, thus distinguishing between sequence length and polydispersity of chains produced in batch and starved-feed semibatch operations; (*iv*) makes possible the screening of products, based on such details as the number and weight fractions of products having different comonomer units located at various positions along the copolymer chains. The aforementioned characteristics were achieved by stochastic calculations through code developed in-house. This KMC simulator becomes a very useful tool for the development of tailored copolymers through free radical polymerization, with blocks separated with single units of a different type.

Keywords: Free radical copolymerization; Starved-feed polymerization; Semibatch polymerization; Kinetic Monte Carlo simulation; Bivariate distribution; Tailored copolymer properties

1. INTRODUCTION

Control of microstructural features of copolymer (or terpolymer) chains in free radical polymerization is not easy and, despite recent advances in mathematical modeling and prediction of copolymer properties, far from perfect. The typical dilemma of batch-to-batch variability is a serious concern: two batches with the same average copolymer composition show different properties and final behavior, depending on the differences between sequential arrangements of monomer units along the respective copolymer chains.

Theoretically, one would be able to manipulate and control the microstructure of the copolymer chains, if one had complete information on the copolymer composition distribution (CCD) and chain length distribution (CLD), both instantaneous and cumulative. However, experimental efforts hardly ever have such complete information, and this makes the practical implementation (of whatever techniques one may devise in order to compensate for this lack of information) quite complicated (e.g., see the procedures, main concepts and background assumptions put forward in references [1] to [10]).

The question still remains: with so many deterministic and stochastic modeling approaches and algorithms, what computational modeling algorithm will offer a satisfactory, yet comprehensive, overview of the polymeric chain detail needed?

In recent studies, we developed a Monte Carlo (MC) computer code capable of giving detailed information on the copolymerization kinetics and microstructural evolution and obtained extremely promising results on chain architectural development [11-13]. It was shown that the kinetic Mote Carlo (KMC) simulation approach can provide sufficient information to predict and better identify events taking place at the molecular level. This undoubtedly demands a detailed computer program with the potential to track a large volume of simulations and necessitates simultaneous control of three important features: (i) the quality of CPU data storage and transfer; (ii) the quality of RAM storage; and (iii) the speed of writing on and/or reading from hard disk drives.

In the current work, we discuss and put into practice the idea of quantifying microstructural changes during copolymerization. For a given system with A and B as

comonomers, there are many possibilities for B units to be arranged in the growing copolymer chains depending on the monomer reactivities and polymerization method. Thus, it would be of premier importance to start from simple and well-understood cases and then move to more complex ones to guarantee generalization to scenarios with, for instance, significant compositional drift. With this in mind, we start with starved-feed semibatch free radical copolymerization where reactivity ratios are set to unity enabling comparison of our model results with those recently reported by Parsa et al. [10]. The developed KMC code satisfactorily enables synthesis and screening in terms of the number and weight fractions of products having different comonomer units located at various positions along the copolymer chains. Comparison of molecular-level features of a starved-feed semibatch with those of a batch process provides sufficient insight into the nature of the former process when one wishes to control the degree of polymerization. The developed code is executed to stochastically produce and screen macromolecules in terms of evolutionary weight distribution and bivariate copolymer composition-chain length (CC-CL) distribution of chains having different numbers (sequences) of B units. We also theoretically tailor copolymer chains, in which B units can take various positions in the growing chain, which will be of vital importance from an engineering angle.

2. MODELING AND SIMULATION

2.1 Model Development and Simulation

The key determining factor in KMC simulation studies is the functionality of the algorithm designed to select the most probable reaction channel, manage the reactants' consumption and products' generation, and update and restore the information of the simulation volume [14-15]. Considering the fact that in copolymerizations macromolecules with various architectural features are produced, an appropriate identification card capable of storing maximum possible topological characteristics of the generated chains should be defined and issued. In addition, the data storage algorithm and corresponding computer code are of vital importance and must be designed to improve the calculation speed of the KMC simulator.

The main advantages of the KMC simulation approach are as follows:

(1) Certain assumptions like the quasi-steady state approximation (QSSA) and long chain approximation (LCA) applied during deterministic modeling of polymerizations are not required in the KMC approach. In other words, the stochastic algorithm

developed in the KMC simulation approach is capable of tracking and recording a comprehensive image of all macromolecular species individually.

(2) While the method of moments results in the averages of molecular weight distribution (MWD) and CCD, the KMC simulation approach is able to predict and construct time-dependent distributions of various molecular characteristics during the course of polymerization.

(3) Despite the fact that many numerical deterministic methods, especially the discrete Galerkin h-p algorithm, are successfully employed in describing polymerizations, they cannot track and record all topological/architectural characteristics of individual macromolecules in the simulation volume. On the other hand, applying the KMC simulation approach, a very specially tailored algorithm and computer code can be developed for any particular polymerization system. Accordingly, the dynamic topological features of all macromolecules inside the simulation volume can easily and individually be visualized in detail.

In the current work, the free radical copolymerization was studied of monomer A and comonomer B, with minimum compositional drift, and copolymers with predetermined chain length and molecular architecture were virtually synthesized applying Gillespie's algorithm [10, 16]. The target microstructure is depicted in Table 1 (Cases I and II) and defined as a linear binary copolymer with chain length of 20 ending in a B comonomer. Case I corresponds to batch operation, whereas Case II is a starved-feed semibatch policy.

Table 1. Molecular architecture of target copolymers

	Target Architecture	**$ASL_n(A)$[1]**	**$ASL_n(B)$[2]**	**$f_{B,optimum}$[3]**
Case I	**AAAAAAAAAAAAAAAAAAB**	19	1	0.053
Case II	**AAAAAAAAAAAAAAAAAAB**	19	1	0.053

1 Average sequence length of "A" units.
2 Average sequence length of "B" units.
3 Optimum mole fraction of "B" component in the feed to meet predetermined architecture.

To produce copolymer chains with minimum compositional drift, the copolymerization scheme and conditions used by Parsa et al. [10] were adopted (see Scheme 1). In the proposed scheme, one can see the initiation, propagation, chain transfer (to monomer and solvent), and termination reaction channels.

(1)	Initiator dissociation	$I \xrightarrow{k_d} 2\,f PR^{\bullet}$
(2,3)	Initiation	$PR^{\bullet} + M_j \xrightarrow{k_i} R^{\bullet}_{1,j}$
(4-7)	Propagation	$R^{\bullet}_{n,i} + M_j \xrightarrow{k_{p,ij}} R^{\bullet}_{n+1,j}$
(8-11)	Chain transfer to monomer	$R^{\bullet}_{n,i} + M_j \xrightarrow{k_{tM,ij}} P_n + R^{\bullet}_{1,j}$
(12,13)	Chain transfer to solvent	$R^{\bullet}_{n,i} + S \xrightarrow{k_{tS}} P_n + PR^{\bullet}$
(14)	Termination by combination	$R^{\bullet}_{n,i} + R^{\bullet}_{m,j} \xrightarrow{k_{tc}} P_{n+m}$
(15)	Termination by disproportionation	$R^{\bullet}_{n,i} + R^{\bullet}_{m,j} \xrightarrow{k_{td}} P_n + P_m$

i , *j*: *A* or *B*

$PR^{\bullet}$: Primary radical

f: Initiator efficiency

I , M_j: Initiator molecule and monomer/comonomer, respectively

$R^{\bullet}_{n,i}$: Macroradical with *n* repeat units ending in *i*-type monomer

P_n : Copolymer chain with *n* repeat units

Scheme 1. Reaction scheme applied to copolymerization [10]

In order to select a macroradical for propagation, a selection probability was assigned to each growing chain present in the simulation volume [11-13]. A random number, *r*, was generated and the m^{th} growing chain of type *h* (terminal monomer unit) was selected for propagation provided the following criterion was satisfied:

$$\sum_{j=1}^{m-1} p_{j,h} \le r < \sum_{j=1}^{m} p_{j,h} \quad , \quad p_{j,h} = \frac{1}{R_h} \tag{1}$$

In this criterion, $p_{j,h}$ is the selection probability of the j^{th} growing chain of type *h* and R_h is the total number of macroradicals of type *h* in the simulation volume. Generally, in linear binary free radical copolymerizations two distinct types of macroradicals, i.e., radicals ending in A or B repeat units, can be recognized in the reaction medium. To propagate the selected growing chain at the given time interval, the selection probabilities of A and B were determined based on the instantaneous propagation reaction rates (relative to the total polymerization rate). In this way, the incorporation probability of monomer and comonomer to the growing chains was precisely determined. Considering the classical statistical copolymerization equations, these probabilities are related to the reactivity ratios and concentrations of monomer/comonomer at that specific moment [17]. The selection mechanism of radical chains to participate in transfer and termination reaction channels is exactly

similar to the aforementioned mechanism employed to simulate the propagation channel.

The number of initial A molecules was chosen as the basis to define and construct the simulation volume. To do this, a total of 10^{12} initial A monomer units was used as the initial input value to the computer code. Considering the initial conditions listed in Table 2, the numbers of initial B molecules, initiator, and solvent molecules were computed accordingly.

Table 2. Copolymerization simulation characteristics [10]

Parameter	**Value**	**Unit**
Solvent (xylene) initial mass	200	g
Total (monomer and initiator) initial mass	500	g
Monomer to initiator molar ratio	20	-
Molecular weight of monomer A	142	g mol^{-1}
Molecular weight of comonomer B	142	g mol^{-1}
Initiator molecular weight	132	g mol^{-1}
Solvent molecular weight	106	g mol^{-1}
Density of monomer A	0.786	g cm^{-3}
Density of comonomer B	0.786	g cm^{-3}
Initiator density	0.885	g cm^{-3}
Solvent density	0.713	g cm^{-3}
Copolymer density	1.078	g cm^{-3}
Target $\overline{DP}_n$	20	-
Copolymerization temperature	138	°C

The algorithm allowed the simulation of a statistically large sample size with a computationally cost-effective execution time. The values of required reaction rate constants were extracted from the literature and are summarized in Table 3 [10].

Table 3. Kinetic characteristics used in copolymerization simulation [10]

Parameter	**Value**	**Unit**
Initiator dissociation rate constant ($\boldsymbol{k_d}$)	1.32×10^{-3}	sec^{-1}
Initiator efficiency ($\boldsymbol{f}$)	0.515	-
Initiation rate constant ($\boldsymbol{k_i}$)	4.69×10^{3}	lit mol^{-1} sec^{-1}
Homo-propagation rate constant (A, $\boldsymbol{k_{p,AA}}$)	4.69×10^{3}	lit mol^{-1} sec^{-1}
Homo-propagation rate constant (B, $\boldsymbol{k_{p,BB}}$)	4.69×10^{3}	lit mol^{-1} sec^{-1}
Reactivity ratio of A ($\boldsymbol{r_A}$)	1	-
Reactivity ratio of B ($\boldsymbol{r_B}$)	1	-
Chain transfer to monomer rate constant ($\boldsymbol{k_{tM,ij}}$)	0.266	lit mol^{-1} sec^{-1}
Chain transfer to Solvent rate constant ($\boldsymbol{k_{tS}}$)	1.66026	lit mol^{-1} sec^{-1}
Termination by combination rate constant ($\boldsymbol{k_{tc}}$)	1.7115×10^{7}	lit mol^{-1} sec^{-1}
Termination by disproportionation rate constant ($\boldsymbol{k_{td}}$)	3.1785×10^{7}	lit mol^{-1} sec^{-1}

2.2 Model for placement of B comonomer in the copolymer chain

In linear binary free radical copolymerizations the arrangement of monomer units along the copolymer chains is dictated by the reactivity ratios and instantaneous concentrations of the monomer and comonomer. Considering the fact that the reactivity ratios are intrinsic characteristics of any set of monomer/comonomer at any given copolymerization conditions, the relative instantaneous concentrations of monomer and comonomer, i.e., initial feed composition, is the main operational factor to adjust their insertion frequency into a growing macroradical. As the instantaneous consumption rates of monomer and comonomer is not the same, the feed composition experiences a continuous change (drift) during the course of copolymerization, which significantly influence the microstructure of the growing copolymer molecules. In other words, copolymer chains with different microstructures are produced at the course of copolymerization if the feed composition drift is not continuously corrected. Hence, to generate architecturally uniform copolymer chains, the feed composition must be precisely adjusted by addition of monomer/comonomer in regular time intervals during the course of copolymerization, except for the ideal random free radical copolymerization case, i.e., when both reactivity ratios are equal to unity.

In this simulation work the reactivity ratios of A monomer and B comonomer are set to be unity, that is the instantaneous feed composition and copolymer composition remain unchanged over the entire copolymerization time. Hence, the initial feed composition is the key factor controlling the architectural properties of the final product and should be precisely evaluated for each predetermined microstructure.

According to the classical statistical free radical copolymerization equations, the instantaneous number average sequence length distribution of monomer and comonomer can easily be obtained as follows [17]:

$$ASL_n(A) = \sum_{i=1}^{\infty} i\,(N_A)_i \tag{2}$$

where $(N_A)_i$ denotes the mole fraction of a sequence of monomer *A* units of length *i* in a linear binary copolymer. More specifically, this represents the number sequence length distribution of monomer *A*, $SLD_n(A)$, and is obtained by calculation of the formation probability of such a sequence:

$$(N_A)_i = (p_{AA})^{(i-1)}\,p_{AB} \quad where: \quad p_{AA} = \frac{r_A f_A}{r_A f_A + f_B} \quad and \quad p_{AB} = 1 - p_{AA} \tag{3}$$

In equation (3), p_{AA} and p_{AB} are the probabilities of a radical chain ending in monomer A to take on an A or B monomer unit, respectively. Moreover, r_A is the reactivity ratio of monomer A, while f_A and f_B are the molar fractions of A and B comonomers in the feed, respectively.

To evaluate the required initial feed composition leading to a predetermined copolymer microstructure (Table 1), the number average sequence length distribution of the target binary copolymer was calculated applying equations 2 and 3. To do this, a computer program was developed to calculate various sequence lengths of A and B applying equation 3. Computing different sequence lengths, the computer code precisely constructs the number SLD of monomer and comonomer. It should be noted that the maximum allowed A and B sequence lengths was set to 10^7, which is physically and statistically large enough to produce reliable and accurate number average sequence lengths. Afterwards, the number average sequence lengths were calculated employing equation 2.

To find an optimum initial feed composition, the computer code calculates the A and B number average sequence lengths for all possible initial feed compositions and compares the results with the A and B number average sequence lengths of the target copolymer. This scanning process was set to be initiated from 0.001 with an increment of 0.001 within the range of all possible feed compositions. It is obvious that the optimum feed composition is the feed composition that results in the identification of a minimum value in the following error function:

$$erF(f_A) = \sum_{i=A,B} \left(ASL_n(i)\big|_{target} - ASL_n(i)\big|_{calculated} \right)^2 \quad (4)$$

This error function determines the difference between the calculated number average sequence lengths and the predetermined values of the target copolymer. The feed composition at the identified minimum is the optimum initial feed composition in synthesizing binary copolymers that have the most similar architecture to the target copolymer. The simulation flow chart searching for the optimum initial feed composition is depicted in Scheme 2.

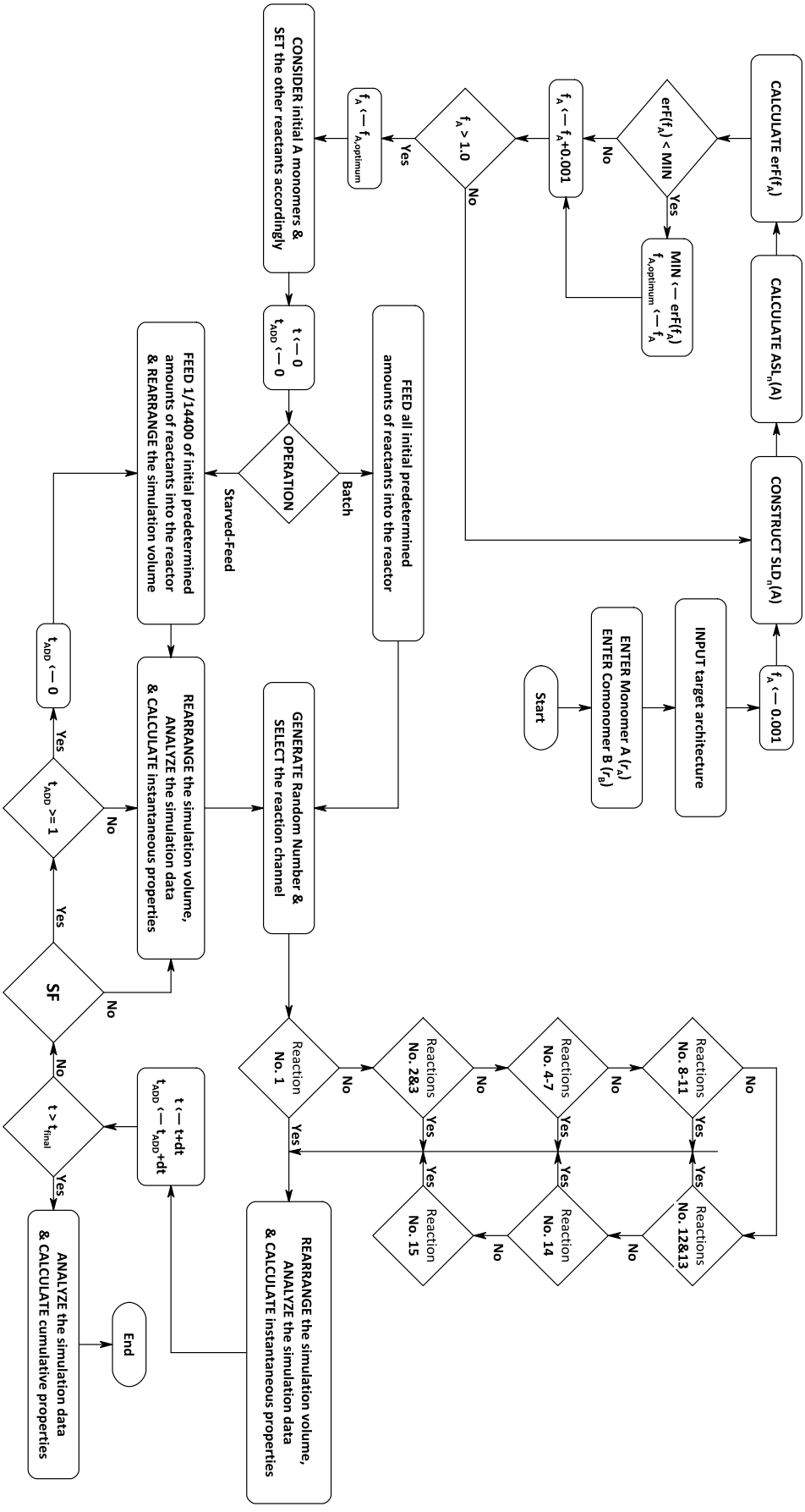

Scheme 2. The simulation flow chart to synthesize binary copolymers

Figure 1 shows the number sequence length distributions of A and B, based on the calculated initial feed composition of the target copolymer cited in Table 1. The calculated optimum value of the initial B mole percent was 5.30 % for both batch and starved-feed semibatch operations.

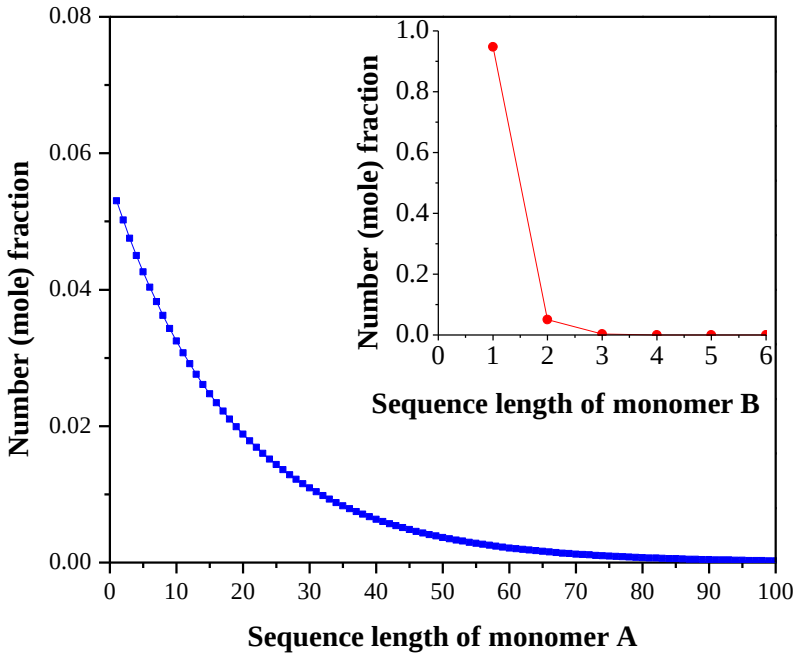

Figure 1. Calculated number sequence length distributions of monomer A, $(N_A)_i$, and comonomer B, $(N_B)_i$, at optimum initial feed composition

The total simulation time used, i.e., the free radical copolymerization reaction time (t_f), was 240 minutes. The computer code can stop the polymerization whenever it encounters monomer or radical depletion.

A computer program, according to the computational algorithm and flow chart presented in Scheme 2, was written in Pascal programming language and compiled into 64-bit executable code using FPC 2.6.2. A subroutine based on the "Mother-of-all Pseudo Random Number Generators" algorithm [18] was exploited to produce the required random numbers for the simulation. The random number generation subroutine satisfied the tests of uniformity and serial correlation with high resolution. The cycle length of the random number generator was 3×10^{47}.

Simulations were performed with a desktop computer with Intel Core i7-3770K (3.50 GHz), 32 GB of memory (2133 MHz), under Windows 7 Ultimate 64-bit operating system. The runtime was approximately 2.46 and 3.27 hours for starved-feed semibatch and batch operations, respectively.

3. RESULTS AND DISCUSSION

As mentioned in the previous sections, the developed model was applied to both batch and starved-feed semibatch operations to capture molecular-level features in the course of free radical copolymerization. To appropriately reflect the ability of the model in anticipating the evolutionary events as well as the difference between batch and starved-feed process, the simulation results are categorized into two subsections. In the first part, we discuss in depth the advantages of the starved-feed semibatch process against batch in terms of statistical patterns revealed by the KMC approach. In the second part, it is shown that the developed model is capable of producing tailored copolymers with different comonomer arrangements along the copolymer chains (a very useful guide for product design).

3.1 Starved-feed semibatch vs. batch copolymerization: Generic features of the KMC algorithm

Figure 2 shows typical operational profiles from starved-feed semibatch and batch processes. Figure 2a demonstrates the variation of the number-average degree of polymerization (DP_n on the left-hand side axis) and polydispersity index (PDI on the right-hand side axis) for a starved-feed semibatch copolymerization process. Figure 2b does the same thing for a batch copolymerization. The insets in both plots show monomer A consumption rate. Figure 2 captures clearly the expected differences between semibatch and batch operation, along with the advantages of the former in both the PDI level and the ability to produce a controlled (and hence predetermined) copolymer chain length. The profiles of Figure 2 can be explained if one looks at the corresponding profiles of Figure 3. Figure 3a shows monomer to initiator molar ratio for a starved-feed semibatch copolymerization (batch process in the inset), whereas Figure 3b plots the ratio of moles of monomer consumed instantaneously (related to monomer consumption rate), d[*M*], to the corresponding total primary radical concentration, [PR^o], for the same cases. One can confirm from Figure 2 and Figure 3b the correspondence between chain length and the ratio of monomer concentration

change to radical concentration. The operational characteristics simulated in Figures 2 and 3 mimic the copolymerizations described in [19].

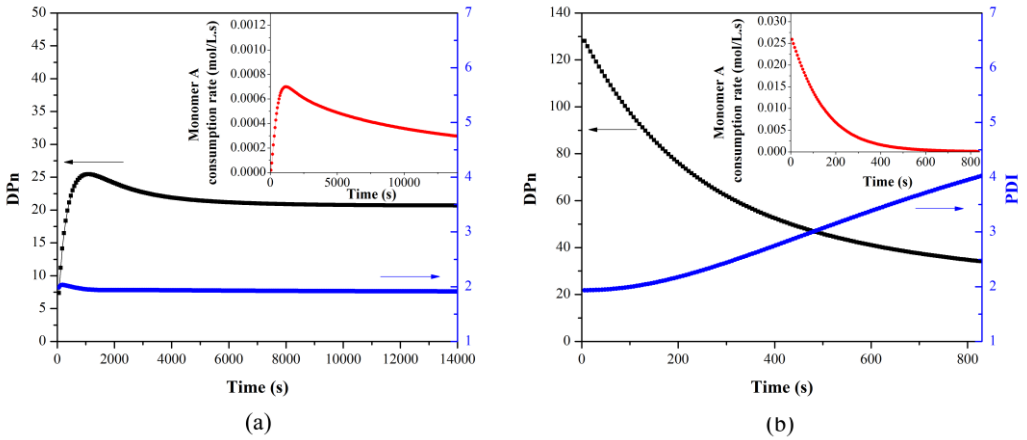

Figure 2. Variation of number-average degree of polymerization (DP_n) and polydispersity index (PDI) of copolymer chains together with monomer A consumption rate (inset) during starved-feed semibatch (a) and batch (b) copolymerization processes

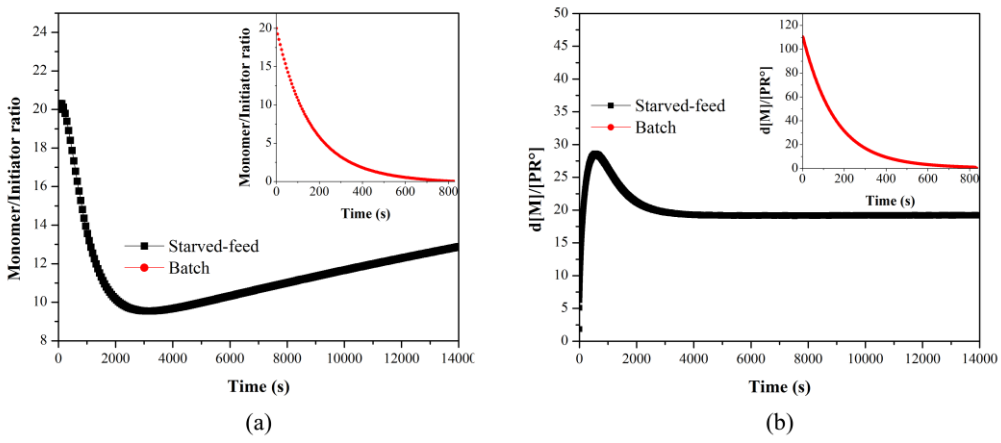

Figure 3. Variation of monomer to initiator molar ratio (a) and moles of monomer consumed to primary radical concentration ratio (b) during the course of starved-feed semibatch and batch (inset) copolymerization processes

With respect to copolymer product quality, Figure 4 shows chain length distribution information (as W(Log(DP)), with W denoting weight fraction and DP degree of polymerization), whereas Figure 5 is related to the sequence length picture. The semibatch strategy results in a narrower chain length distribution (Figure 4) and a

narrower sequence length distribution of A units (Figure 5). The curves overlap in the case of sequence length distribution of B units (Figure 5, inset).

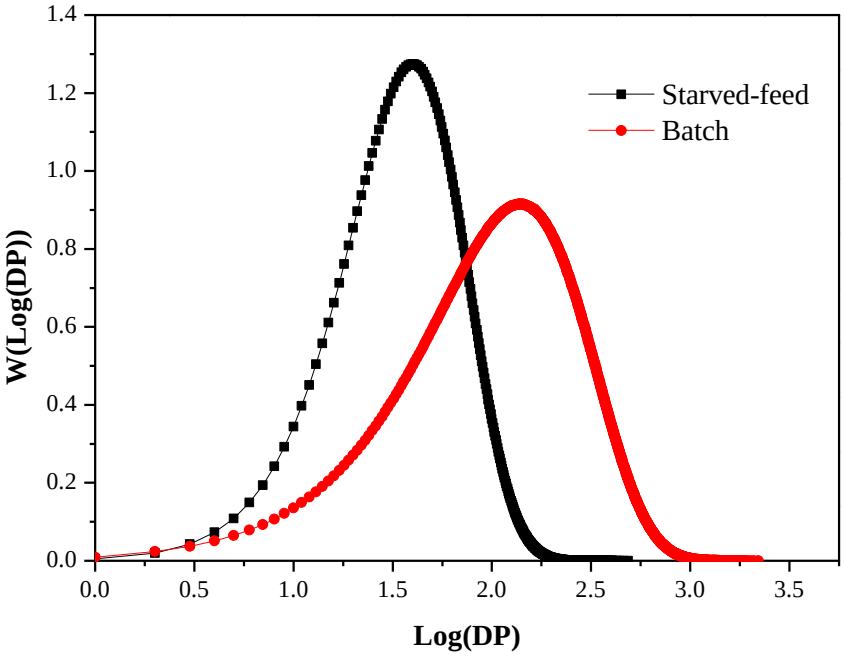

Figure 4. Distribution of copolymer chain length produced via batch and starved-feed semibatch copolymerization routes

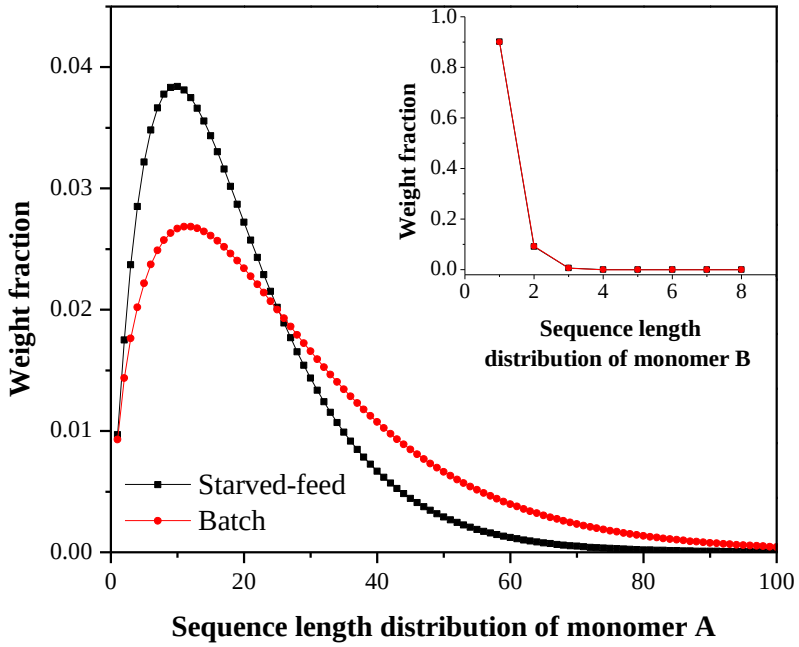

Figure 5. Distribution of A and B (inset) sequence lengths in the copolymer product of batch and starved-feed semibatch copolymerization

Figures 6 and 7 show several more operational characteristics and comparisons between the starved-feed semibatch and batch copolymerization processes. The profiles are all reasonable and shed light on the behavior of the two types of reactor operation. Figure 7 is a confirmation of the reasonable performance of the developed KMC algorithm. Figure 8 confirms that the semibatch operation yields higher productivity (its polymer concentration is 1.6 times higher than the corresponding batch one), while at the same time maintains the average chain length on target (see Figure 2).

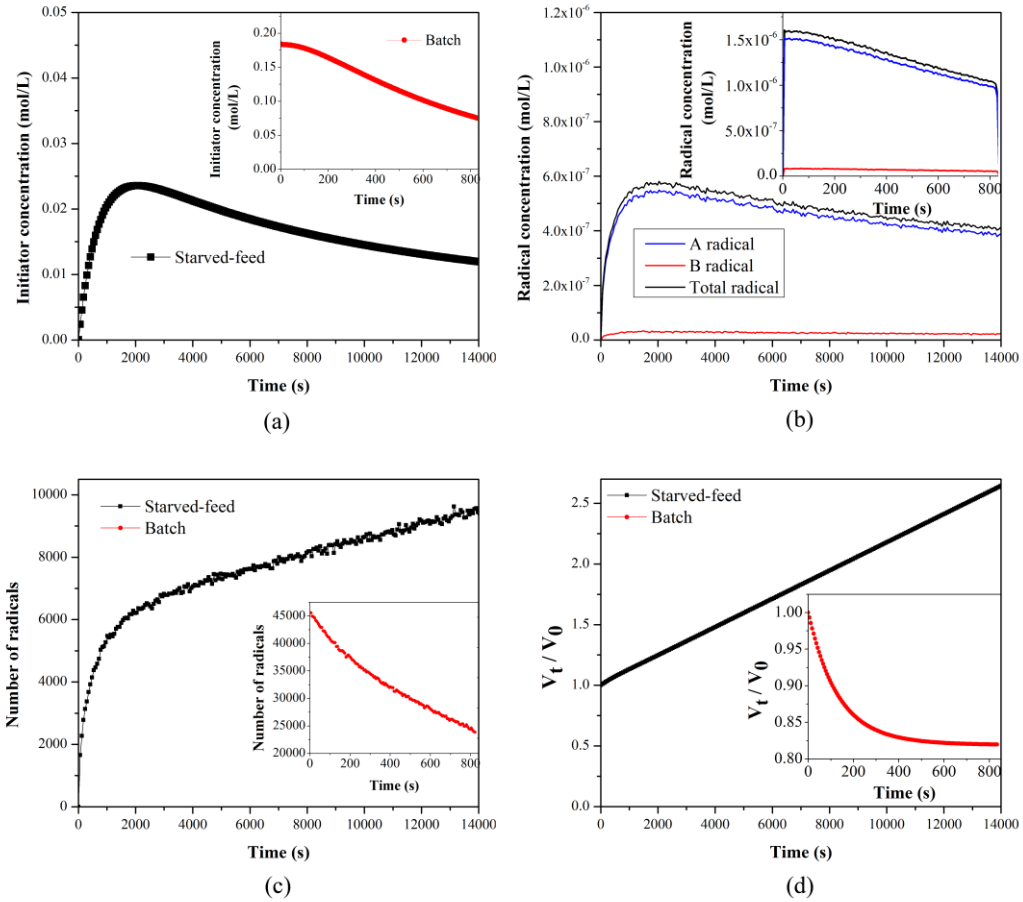

Figure 6. Variation of (a) initiator molar concentration, (b) concentration of radicals A and B, and their total concentration, (c) total number of radicals, and (d) ratio of reaction volume over its initial value in the course of starved-feed semibatch and batch (inset) copolymerization processes

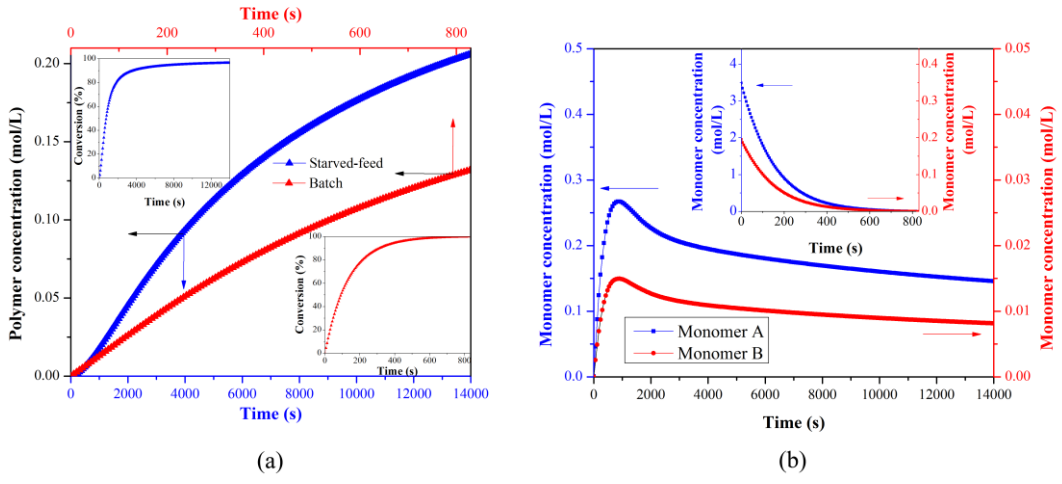

Figure 7. Variation of (a) polymer concentration and conversion (insets) in the course of starved-feed semibatch and batch methods; (b) concentration of monomers in the course of starved-feed semibatch and batch (inset) copolymerization processes

3.2 Starved-feed semibatch vs. batch copolymerization: Advanced features of the KMC algorithm

After the generic features of the KMC algorithm (essentially, after confirming that the developed KMC algorithm can reasonably capture typical features of semibatch and batch copolymerizations) in the previous subsection, a discussion of several advanced features of the KMC approach is now in order. One can now employ the KMC algorithm to produce copolymer molecules with tailored microstructures and track the evolution of weight fraction patterns in terms, for instance, of the number of B units per copolymer chain, or follow the bivariate chain length/copolymer composition distribution. These can be performed in cases where the quasi-steady-state-assumption (QSSA) for radicals and the long-chain-approximation (LCA) are not valid, and also without any other simplifications commonly used, as described in [8, 20].

The developed KMC simulator can fractionate, based on the number and weight of molecules, all the produced copolymer chains having 0, 1, 2, 3 … and n B units along the copolymer chain. In each case, it was also possible to predict the placement of B comonomer units in the copolymer chains, which made it possible to architecturally fractionate the copolymers having n B units based on the number and/or weight of fragments. Figure 8 compares the time varying weight fraction distributions of copolymers having different degrees of incorporation of B units per chain obtained in the simulation of batch and starved-feed semibatch processes. These plots are illustrative of the evolution of copolymer chains having n B units in their backbone and offer more insight in the state of each process for different operating conditions. For example, homopolymer molecules of type A increasingly populate the batch system over reaction time (see Figure 8a), while the corresponding product resulting from the starved-feed semibatch operation (see Figure 8b) follows a different trend, in which the weight fraction of homopolymer molecules of type A declines over time. It is also possible to compare cases based on the chain length of the copolymer molecules obtained at the end-of-batch (see Figure 9). In the batch process, the growing chains captured about 94 B units in the copolymer chain, and a wide range of copolymer chains having different number of comonomer units were produced. On

the other hand, the starved-feed semibatch process was successful in controlling the number of B units with a maximum of 27 B units per chain, which is characteristic of a well-controlled chain length in such operations.

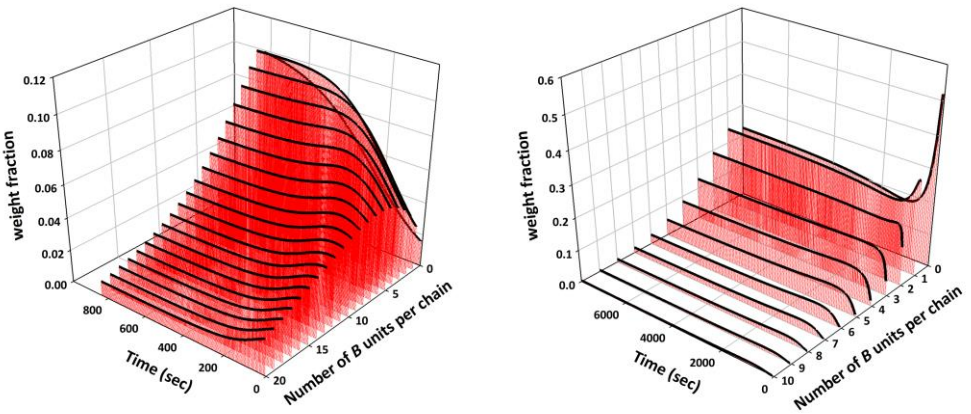

Figure 8. Time varying weight fraction distributions of copolymer chains with different B units per chain produced via (a) batch and (b) starved-feed semibatch copolymerization

The KMC simulation algorithm was also capable of describing the bivariate molecular weight-copolymer composition distribution (see Figure 9). The weight distribution of copolymers having specified B units is obviously narrower in the case of starved-feed semibatch copolymerization; meanwhile the potential of such a system in producing copolymer chains with more than 5 B units in the growing copolymer chain is indeed limited. Another important feature would be the well-controlled length of copolymers produced in the case of starved-feed semibatch copolymerization (see contour plots in Figure 9b). The results of Figure 9 will be further clarified with the two tables that follow (Tables 4 and 5) and the corresponding case studies they describe (Case I (batch) and Case II (semibatch); see also Table 1).

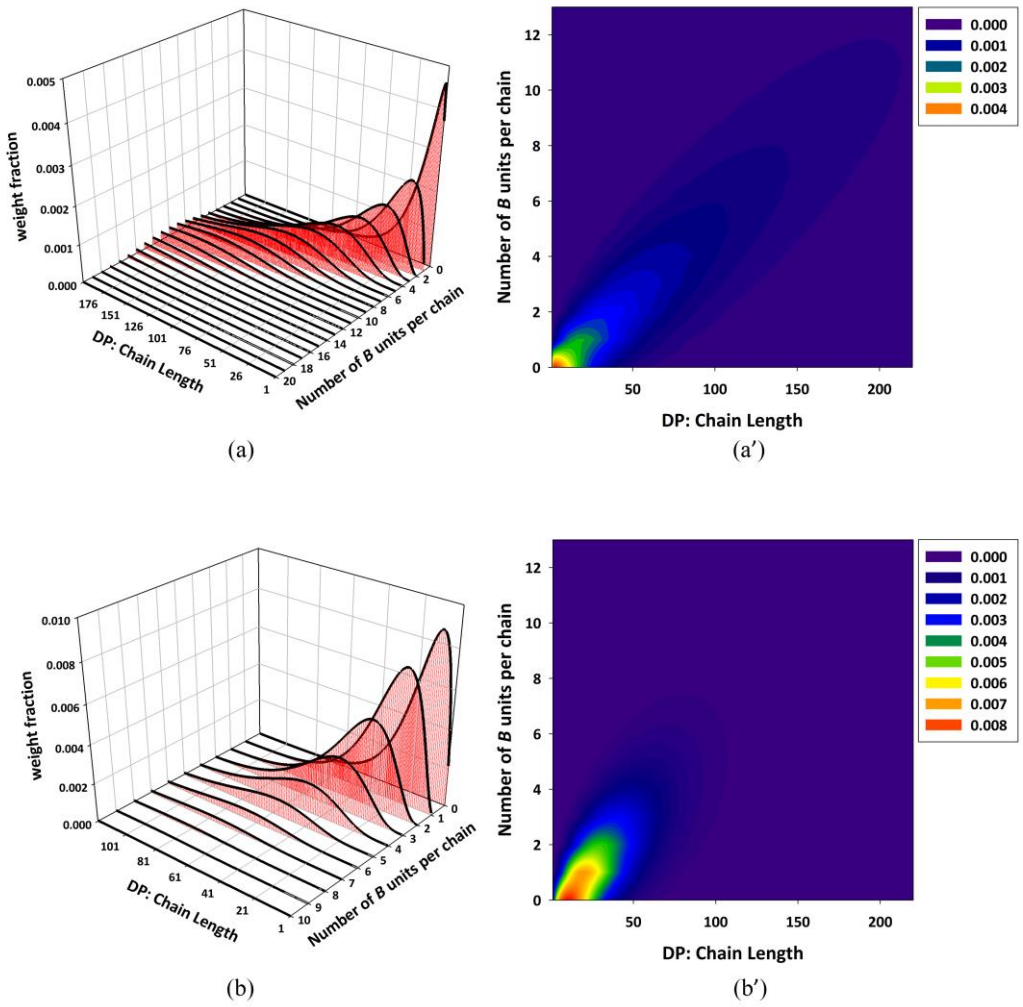

Figure 9. Weight fraction distributions (normal letters) and corresponding contour plots (primed letters) of chains with different lengths comprising varying number of B units per chain produced via (a, a') batch, and (b, b') starved-feed semibatch copolymerization. Colour codes in (a') and (b') refer to the weight fraction of chains.

Tables 4 and 5 compare the copolymer chains produced in Cases I and II, respectively, and give more details based on the differences between number fractions, sequence lengths, and polydispersity values of different chains obtained from the two different operations.

Table 4. Mole fractionation of copolymer chains based on the number of B units, molecular architecture, and differences between sequence length and polydispersity of chains virtually produced in batch (Case I, see Table 1)

CASE I		**B units located at chain ends**				
Number of B per chain	**Number-fraction (%)**	**No end unit (%)**	**One end (%)**	**Both ends (%)**	**DPn**	**PDI**
0	50.3078	50.3078	0	0	18.4015	1.8453
1	18.8406	13.9205	4.9201	0	33.9728	1.4727
2	9.1646	7.4882	1.5584	0.1179	50.4107	1.3139
3	5.6162	4.7346	0.8384	0.0432	66.8866	1.2347
4	3.7953	3.2429	0.5292	0.0232	83.4081	1.1874
5	2.7258	2.3468	0.3637	0.0153	99.9088	1.1565
6	2.0141	1.7431	0.2611	0.0099	116.4229	1.1339
7	1.5299	1.3269	0.1956	0.0073	132.8309	1.1173
8	1.1802	1.0277	0.1472	0.0054	149.4518	1.1041
9	0.9264	0.8072	0.1148	0.0044	165.6778	1.0939
10	0.7320	0.6389	0.0899	0.0032	181.9996	1.0852
11-94	3.1671	2.7738	0.3801	0.0132	-	-

Table 5. Mole fractionation of copolymer chains based on the number of B units, molecular architecture, and differences between sequence length and polydispersity of chains virtually produced in starved-feed semibatch (Case II, see Table 1)

CASE II		**B units located at chain ends**				
Number of B per chain	**Number-fraction (%)**	**No end unit (%)**	**One end (%)**	**Both ends (%)**	**DPn**	**PDI**
0	46.0504	46.0504	0	0	19.3560	1.4894
1	26.4155	21.5145	4.9010	0	28.8156	1.3259
2	13.5663	11.0301	2.4059	0.1302	38.5531	1.2397
3	6.9143	5.6126	1.2339	0.0678	48.3118	1.1899
4	3.5082	2.8446	0.6292	0.0344	58.0512	1.1566
5	1.7697	1.4327	0.3195	0.0175	67.8135	1.1338
6	0.8882	0.7183	0.1608	0.0089	77.5557	1.1161
7	0.4448	0.3603	0.0799	0.0046	87.5621	1.1030
8	0.2225	0.1796	0.0406	0.0023	97.1144	1.0936
9	0.1107	0.0897	0.0199	0.0011	107.2298	1.0857
10	0.0550	0.0444	0.0101	0.0006	116.9506	1.0783
11-27	0.0544	0.04390	0.0100	0.0005	-	-

Scrutinizing the entries of Tables 4 and 5 illustrates that copolymer chains produced in the batch process show, in general, more diversity in the number of B units per chain. A similar trend can be seen in the average degree of polymerization. In spite of the large difference in the number of B units per chain (94 for batch and 27 for starved-feed semibatch), the mole fraction of A homopolymer molecules in each case has remained almost the same. In contrast, the polydispersity index of A homopolymer molecules from the starved-feed process is lower. A comparison

between chains with 1 or 2 B units per chain also shows a difference between the two cases. Another important output of the developed simulator is concerned with the positioning of B units in each case. This can be clearly observed by comparing, for instance, the chains having 2 B units. In the batch process, the number-fraction of these chains is about 9.1% (see Table 4, 3rd row). Among these copolymer chains, approximately 7.5% contain no B units at the end of the grown chains, 1.5% have 1 B unit at the chain ends, and 0.11% have 2 B units at both ends of each chain. On the other hand, the corresponding values in the starved-feed semibatch case (see Table 5, 3rd row again) are respectively calculated by the KMC algorithm as 13.5, 11, 2.4, and 0.13%. Such detailed information is of critical importance in view of applications of synthesized macromolecules. Detailed information on the positioning of comonomer B along the copolymer chains associated with the ability to screening copolymer chains in terms of mole (or weight) fraction could bring more insights into the nature of addition of monomer units in the course of a typical free radical copolymerization, thus leading to tailored macromolecules and essentially guaranteeing predetermined characteristics. This is the topic of the subsection that follows.

3.3 Additional advanced features of KMC: Positioning of B comonomer in the copolymer chains

Table 6 shows four target architectures (Cases III to VI) having different target characteristics to be simulated in the starved-feed (SF) semibatch process. In all cases, the target copolymer chain length was set to 20, where one, two, three, and four B units were allowed to enter the chains of cases III to VI, respectively. Also, no B units were allowed to appear in the chain ends.

Table 6. Molecular architecture of target copolymers expected from starved-feed (SF) semibatch operation

	Process	Target Architecture	$ASL_n(A)$	$ASL_n(B)$	$f_{B,optimum}$
Case III	SF	**AAAABAAAAAAAAAAAAAAA**	9.5	1	0.105
Case IV	SF	**AAAAABAAAAAAAAABAAAA**	6.0	1	0.167
Case V	SF	**AABAAAAABAAAABAAAAAA**	4.25	1	0.235
Case VI	SF	**AABAAABAAAABAAAABAA**	3.2	1	0.312

Figure 10 compares the evolution of weight fraction of simulated copolymer chains having different B units per chain corresponding to the various architectures defined

in Table 6. As the number of B units in the copolymer chains increases going from Case III to Case VI (and from Figure 10a to 10d), the weight fraction of copolymer chains having more B units increases significantly. In addition, the weight fraction distributions of the aforementioned target molecules with the corresponding contour plots are compared in Figure 11. The obtained patterns show peaks at higher chain lengths as the number of B unit increases (moving from case III to VI and Figure 11a to Figure 11d, respectively).

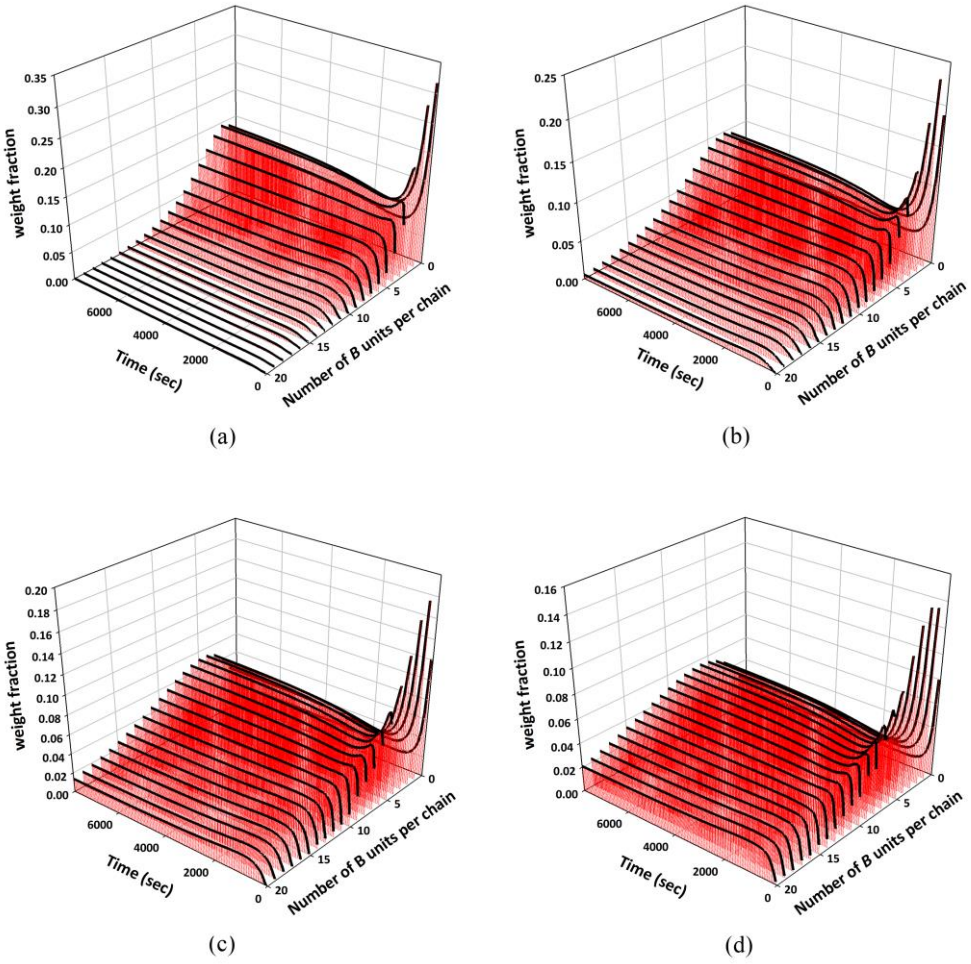

Figure 10. Time varying weight fraction distributions of copolymers with different B units per chain corresponding to cases III (a), IV (b), V (c), and VI (d) described in Table 6

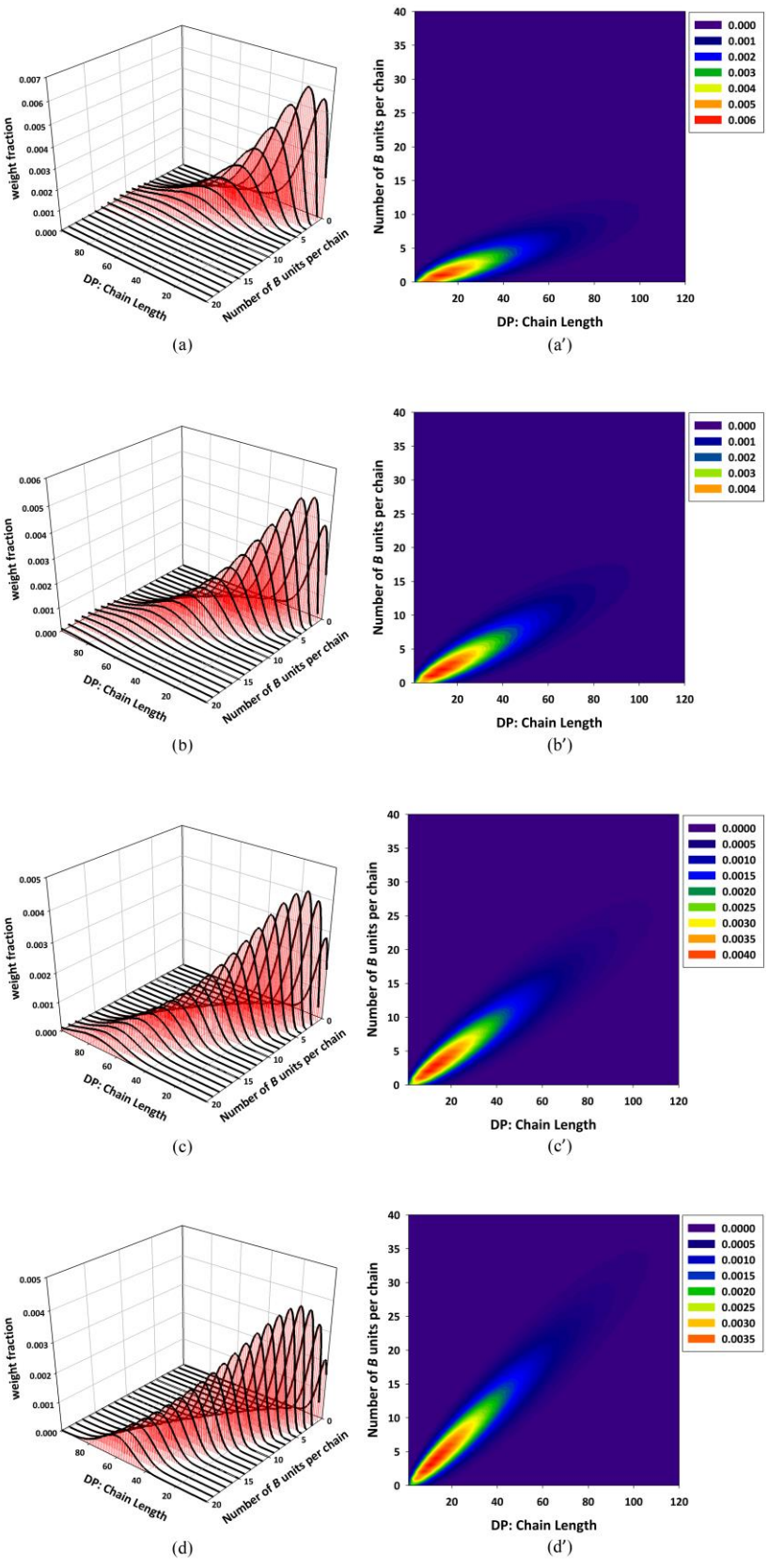

Figure 11. Weight fraction distributions (normal letters) and corresponding contour plots (primed letters) of target copolymers with different B units per chain for cases

III (a, a'), IV (b, b'), V (c, c'), and VI (d, d') of Table 6. Colour codes in (a'- d') refer to the weight fraction of chains.

Detailed features of these copolymer chain architectures are available by the KMC simulator for screening copolymer chains based on their bivariate distribution plots. These are summarized and compared in Table 7.

Table 7. Architectural developments of the cases of Table 6 and the corresponding number and weight fractions of different comonomer placements

Case No.	**Case III**	**Case IV**	**Case V**	**Case VI**
Chains having no B (mol%)	28.8245	19.1050	13.3379	9.4187
Chains having no B (wt%)	9.51402	4.4992	2.3888	1.3262
Chains having no B at the ends (mol%)	80.5415	70.0478	59.3664	48.3368
Chains having no B at the ends (wt%)	80.1217	69.4277	58.5674	47.3749
*Chains with only one B at one end (mol%)	6.2754	6.8753	7.0895	7.0833
*Chains with only one B at one end (wt%)	2.2099	1.7663	1.4144	1.1328
*Chains with only two B at both ends (mol%)	0.3375	0.6121	0.9206	1.2714
*Chains with only two B at both ends (wt%)	0.1274	0.1736	0.2093	0.2404
**Chains with at least one B at the end (mol%)	18.4096	27.2961	35.3702	42.3889
**Chains with at least one B at the end (wt%)	18.7790	27.7946	35.9249	42.9150
**Chains with at least two B at the end (mol%)	1.0489	2.6561	5.2634	9.2744
**Chains with at least two B at the end (wt%)	1.0993	2.7778	5.5078	9.7101
Target microstructure (mol%)	**16.8075**	**9.1055**	**5.5404**	**3.4756**
Target microstructure (wt%)	**11.8542**	**6.8460**	**4.2234**	**2.6085**

*having no B unit at the middle
** having some B units at the middle

A few comments are now in order on the entries of Table 7, for illustrating how useful the information of Table 7 is with respect to delivering a controlled microstructure and desired product for different applications. According to the results obtained in Table 7, 28.82 mole% (equivalent of 9.51 wt%) of the virtually synthesized chains have no functionality (i.e., they include zero B units) in case III. On the other hand, 80.54 mol% (equal to 80.12 wt%) of the produced chains possess no B unit at the ends of chains. Also, case III results in copolymer chains from which 6.27 and 0.34 mole% have exactly one and two B unit(s) located at the end(s) of the chains, respectively. More interestingly, in Case III, 18.41 and 1.05 mol% of chains have at

least one and two functional end(s), respectively. The other outstanding feature of the developed model is related to the difference between target macromolecules in molar or weight fractions. It is evident that the optimal feed composition satisfying production of copolymer chains having two B units placed in the middle of the chain reduces, as expected, the contribution of homopolymerization (chains with zero B units) from 28.82 mole% in case III to 19.10 in case IV. This trend will continue, reaching 13.33 and 9.41 mole fractions for cases V and VI, respectively. Similarly, the percentage of copolymer chains possessing no B units located at the chain ends will fall from 80.54 to 48.33 mole% moving from case III to VI. On the other hand, the contribution of chains possessing exactly one B at one end or those having only two B units located at both ends of the copolymer chains shows a very slight increase in mole fraction from 6.27 to 7.08, and from 0.33 to 1.27, respectively. This means that the contribution of such architectures to the total number or weight of produced copolymer chains is low. In turn, comparison of cases III to VI reveals a significant difference in the mole or weight fraction of chains having at least one or two B units situated at the ends. Interestingly enough, it can be seen that even when applying an optimal feed to the starved-feed semibatch process, the percentage of target macromolecules is still low and follows a decreasing trend from 16.80 to 3.47 mol% (11.85 to 2.60 wt%) as we move from case III to IV. Since production of target macromolecules through the starved-feed semibatch free radical copolymerization is associated with development of copolymer chains having less or more B units than those desired, the comparison of weight fraction distributions of copolymers having n B units in their backbone and those having specified B units all situated at the middle of the copolymer chains can be very informative (see Figure 12). It is obvious that increasing the number of B units widens the weight fraction distribution of copolymer chains having different number of comonomers. Despite the fact that production of polymers with controlled chain length is the characteristic of a starved-feed process, the diversity of copolymer chains in view of B units incorporated into the growing chains should be taken into equal consideration. The distribution of copolymers having n B units at the middle peaks at around the number of B units in the target macromolecule (see inset plot in Figure 12). To conclude, the differences between target cases should be analyzed in view of the detailed information provided in either Table 7 or Figure 12. It is to be noted that the developed code can appropriately capture fluctuations in the architecture of growing chains when reactivity ratios are

not equal to unity, which will be the subject of a future investigation, and which will offer additional insights into the nature of comonomer addition and positioning.

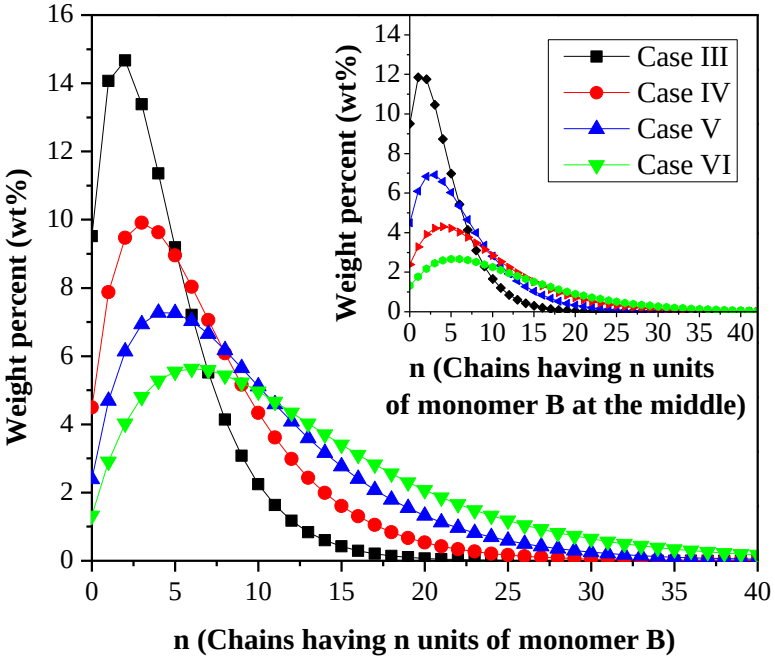

Figure 12. Weight fraction distributions of chains having n B units and those possessing n B units placed at the middle (inset plot) for the different target copolymers of Table 6

4. CONCLUSION

We introduced an algorithm based upon a Kinetic Monte Carlo (KMC) simulation approach capable of quantifying the architectural evolution of chains during starved-feed semibatch free radical copolymerization, through which a large number of copolymer chains was produced, screened, and analyzed in a computationally cost-effective manner. The developed model was implemented on either batch or starved-feed semibatch operations with an optimized feed. This optimized feed enabled achieving microstructures exhibiting prespecified number and sequence length distributions of comonomers with a minimum deviation from target copolymer chains. Comparisons of evolutionary trends in the average degree of polymerization, polydispersity index, chain length distribution, and the rate of different reaction pathways confirmed the uniformity of copolymer chains produced through starved-

feed operations (and yielded the expected Flory-Shultz distribution patterns). Three-dimensional plots corresponding to time varying weight fraction distributions of copolymers having different degrees of incorporation of B comonomer units per copolymer chain revealed populations of homopolymers in the batch system, whereas the starved-feed operation achieved optimal results as per the different targets. The detailed information obtained on the chain architectures, including the number and weight fractions of chains having n B units together with different positioning (placement) of the comonomer units, e.g., chains with zero, one or two B comonomer(s) located at the end(s), shed light on the many different and useful features of the developed MKC computer code in tracking the detailed architectural development of the different copolymer chains during the course of starved-feed semibatch copolymerization.

REFERENCES

1. M. S. Montaudo, *Macromolecules* **2001**, *34*, 2792.
2. M. M. Khorasani, M. R. Saeb, Y. Mohammadi, M. Ahmadi, *Chem. Eng. Sci.* **2014**, *111*, 211.
3. K. Matyjaszewski, N. V. Tsarevsky, *J. Am. Chem. Soc.* **2014**, *136*, 6513.
4. H. Tobita, *Macromol. Theory Simul.* **2014**, *23*, 182.
5. W. Wang, R. A. Hutchinson, *Macromolecules* **2008**, *41*, 9011.
6. E. Mavroudakis, K. Liang, D. Moscatelli, R. A. Hutchinson, *Macromol. Chem. Phys.* **2012**, *213*, 1706.
7. W. Wang, R. A. Hutchinson, *Macromol. Symp.* **2010**, *289*, 33.
8. W. Wang, R. A. Hutchinson, *AIChE J.* **2011**, *57*, 227.
9. Y. Zhao, Y. W. Luo, C. Ye, B. G. Li, S. Zhu, *J. Polym. Sci., Part A: Polym. Chem.* **2009**, *47*, 69.
10. M. A. Parsa, I. Kozhan, M. Wulkow, R. A. Hutchinson, *Macromol. Theory Simul.* **2014**, *23*, 207.
11. Y. Mohammadi, M. Ahmadi, M. R. Saeb, M. M. Khorasani, P. Yang, F.J. Stadler, *Macromolecules* **2014**, *47*, 4778.
12. Y. Mohammadi, A. S. Pakdel, M. R. Saeb, K. Boodhoo, *Chem. Eng. J.* **2014**, *247*, 231.
13. M. R. Saeb, Y. Mohammadi, M. Ahmadi, M. M. Khorasani, F. J. Stadler, *Chem. Eng. J.* **2015**, *274*, 169–180.

14. H. Xi, R. Hentschke, *Macromol. Theory Simul.* **2014**, *23*, 373.

15. Y. R. Zhao, K. B. McAuley, P. D. Iedema, J. E. Puskas, *Macromol. Theory Simul.* **2014**, *23*, 383.

16. M. Fluendly, *Markov Chains and Monte Carlo Calculations in Polymer Science*, Marcel Dekker: New York, 1970; p 45.

17. G. Odian, *Principles of Polymerization*, 4th ed.; Wiley-Interscience: New York, 2004; p 481.

18. G. Marsaglia, *J. Modern Applied Statistical Methods* **2003**, 2 (1), 2.

19. K. F. O'Driscoll, A. F. Burczyk, *Polym. React. Eng.* **1993**, *1*, 111.

20. W. Wang, R. A. Hutchinson, M. C. Grady, *Ind. Eng. Chem. Res.* **2009,** *48*, 4810.